



Interferometric delay tracking for low-noise Mach-Zehnder-type scanning measurements

WOLFGANG SCHWEINBERGER,^{1,2,*} LENARD VAMOS,^{3,4} JIA XU,³ SYED A. HUSSAIN,^{1,3} CHRISTOPH BAUNE,⁵ SEBASTIAN RODE,⁵ AND IOACHIM PUPEZA^{1,3,6}

¹Ludwig-Maximilians-Universität München, Am Coulombwall 1 85748 Garching, Germany

²King Saud University, Department of Physics and Astronomy, Riyadh 11451, Saudi Arabia

³Max-Planck-Institut für Quantenoptik, Hans-Kopfermann-Straße 1 85748 Garching, Germany

⁴ICFO -The Institute of Photonic Sciences, Mediterranean Technology Park, Av. Carl F. Gauss 3 08860 Castelldefels (Barcelona), Spain

⁵SmarAct GmbH, Schütte-Lanz-Straße 9 26135, Oldenburg, Germany

⁶ioachim.pupeza@mpq.mpg.de

*w.schweinberger@lmu.de

Abstract: Precise delay control is of paramount importance in optical pump-probe measurements. Here, we report on a high-precision delay tracking technique for mechanical scanning measurements in a Mach-Zehnder interferometer configuration. The setup employs a 1.55- μm continuous-wave laser beam propagating along the interferometer arms. Sinusoidal phase modulation at 30 MHz, and demodulation of the interference signal at the fundamental frequency and its second harmonic, enables delay tracking with sampling rates of up to 10 MHz. At an interferometer arm length of 1 m, root-mean-square error values of the relative delay tracking below 10 attoseconds for both stationary and mechanically scanned (0.2 mm/s) operation are demonstrated. By averaging several scans, a precision of the delay determination better than 1 as is reached. We demonstrate this performance with a mechanical chopper periodically interrupting one of the interferometer arms, which opens the door to the combination of high-sensitivity lock-in detection with (sub-)attosecond-precision relative delay determination.

© 2019 Optical Society of America under the terms of the [OSA Open Access Publishing Agreement](#)

1. Introduction

Ultrafast pump-probe measurements such as attosecond streaking [1,2] or THz-TDS [3,4] require precise time-delay measurements, sometimes with a precision down to a few attoseconds [5]. In addition, a long scan range is also necessary to follow the reactions in the case of attosecond streaking or for the study of molecular rovibrational signals with high spectral resolution and accuracy, particularly gaseous samples in time-domain spectroscopy. Therefore, it is mandatory to measure over a long time-range with a sufficiently short time-step with high precision and repeatability [6].

The conventional method for delaying in time-resolved pump-probe experiments is moving a retro-reflector mounted on a mechanical delay stage. At each step the position is held and the corresponding signal is processed (step-scan technique), or the average of several scans with higher speeds is calculated (rapid-scan technique). The position of the stage is determined by a linear encoder of the delay stage typically with 20 nm precision or by utilizing a Michelson interferometer for more precise position detection down to a few nanometers. The step-scan technique is well-known and widely used in most pump-probe methods and its drawbacks have been deeply investigated [7]. An analysis of the noise sources in THz-TDS is given in [8]. Low frequency intensity noise has been addressed in several pump-probe measurements like in THz-TDS and can be suppressed by a lock-in amplifier (LIA), where the THz beam is modulated (most commonly amplitude modulation

by mechanical chopping) and the local oscillator (probe signal) is measured after a nonlinear optical interaction. Typically, the intensity noise of the local oscillator can be suppressed by 100 dB after the demodulation and proper filtering [7].

In this paper we focus on the real-time measurement and reduction of delay time uncertainties, for example stochastic and periodic fluctuations [9] originating from different sources such as refractive index fluctuations of air, airflow turbulences caused by the chopper wheel, and periodic sampling errors from acoustic vibrations and nonlinear movement of the opto-mechanical elements in particular the linear stage.

Several efforts have been made to avoid moving mechanical components in pump-probe setups. One proposed solution is an acousto-optical delay line with 15 as precision over the available time-delay window of 6 ps [10]. Another technique, asynchronous dual-comb spectroscopy, is ideal for rapid scans with tremendous spectral resolution as the repetition rate of the oscillators determines the time-delay window (from 100 ps up to several nanoseconds), and the frequency difference of the two phase-locked oscillators the scanning speed. However, the theoretical time resolution is limited due to residual timing jitter between the two lasers. In state-of-the-art systems, the time-delay fluctuations could be reduced down to 45 fs by active electronic stabilization of the laser frequencies over a time-delay window of 1 ns [3]. Other advanced scan methods in THz-TDS are based on single-shot techniques which encode the pump induced temporal dynamics into the spatial profile of the probe beam, or into the temporal profile of the chirped optical probe beam [11]. The drawbacks are the limited time-delay window determined by the expanded beam size or the length of the chirped probe pulse. For precision Fourier-transform infrared spectrometry (FTIR) measurements, birefringent delay lines provide: attosecond precision for short delay scans [12,13], increased robustness and position accuracy and can be combined with an LIA as shown in [14].

Nevertheless, delay stages are still commonly used because of their simplicity, low cost and universality. A technical solution, widely implemented in commercial FTIR devices, consists of a pilot beam from a frequency-stabilized HeNe laser propagating through the Michelson interferometer of the FTIR. The interferometrically detected position fluctuations are then actively corrected by a piezo-actuated mirror. Timing jitter of less than 20 as can be achieved through application of an active interferometric delay stabilization scheme [5], mainly limited by the locking bandwidth and quality of the feedback loop. Furthermore, it is necessary to take into account the beam pointing instability, caused by the piezo actuator, especially for long beam arms. In THz-TDS, active interferometric delay stabilization has been demonstrated to measure THz absorption spectra up to 5 THz (corresponding to 200 as time delay precision) with 2 fs timing jitter of the THz signal in a fixed signal maximum position over a 10 minute measurement interval [5,15].

In this paper, we propose and characterize an interferometric delay tracking (IDT) method for accurate and real-time delay corrections in pump-probe setups using conventional delay stages and heterodyne measurements with LIA. We employ a commercially available interferometer for position measurements with precision down to a few pm. This interferometer was adjusted for a Mach-Zehnder interferometer (MZI) type test setup, which can be implemented in many general pump-probe arrangements, provided that there is a common path between the pilot, pump and probe beams. Instead of active delay correction (usually limited in bandwidth to few tens of kHz), the tracked position data (acquired at a rate of up to several hundreds of kHz) is used directly for the correction of the nominal delay values in the data processing. The reproducibility of the position measurements is characterized with and without the chopper wheel, demonstrating the robustness of the method and highlighting the noise contributions introduced by the chopper wheel due to generated airflow turbulences.

2. Experimental setup

2.1 Optical layout

The experimental setup consists of an MZI as shown in Fig. 1. The two arms (approx. 1 m long each) are defined by 50/50 beam splitters. For mechanical scanning, a servo-motor-driven linear stage (LS110 from PI miCos GmbH) was included in the delay line. The maximum scan range amounts to 90 mm, corresponding to a ~ 300 ps time window. A commercially available Michelson-interferometer for displacement measurements (SmarAct PicoScale [16]) was implemented for tracking the position of the delay line. The light source is a pig-tailed distributed-feedback (DFB) laser diode emitting a $1.55\text{-}\mu\text{m}$ wavelength continuous-wave (CW) beam, connected via a single-mode fiber to a compact, monolithic Michelson-type sensor head. Here, the laser light is split by a beam splitter cube and one of the outputs is reflected by a coated surface of the cube, serving as the reference arm. The other beam, forming the measurement arm of the Michelson interferometer, is guided to the tracked object, reflected and recombined with the reference beam in the cube. The resulting interference signal is guided back through the optical fiber, measured and the electronic signal is then evaluated inside a controller to infer the object's displacement [16]. This configuration, tracking only the stage movement, serves as a reference for our measurement (channel 2, CH2).

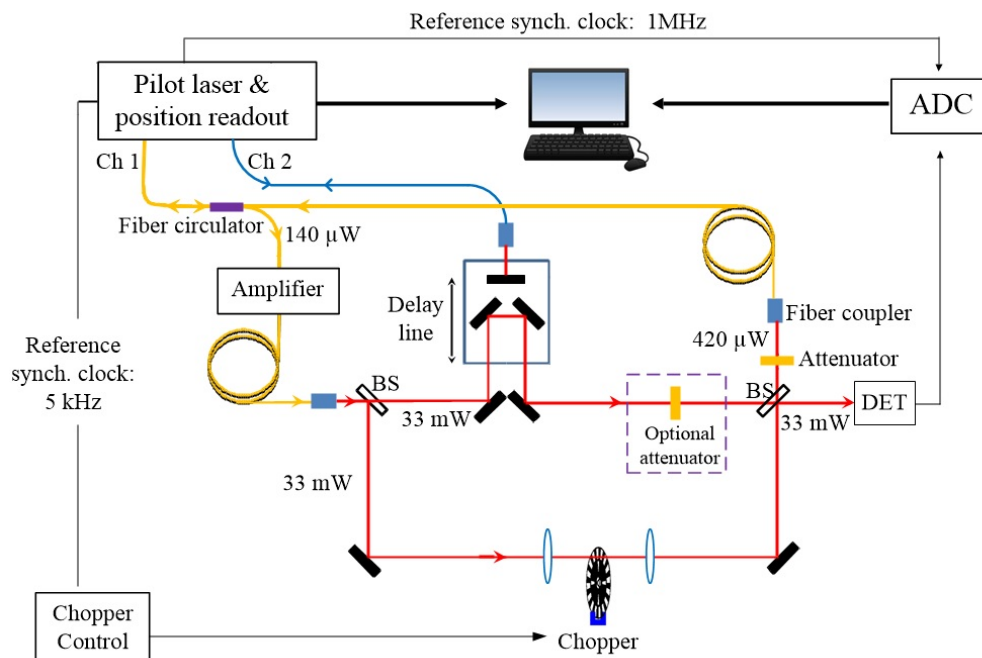


Fig. 1. Test setup: A modified, Mach-Zehnder type position tracking interferometer (channel 1, CH1) is operated in parallel to a commercial Michelson-type sensor head (channel 2, CH2), which monitors the position of a mirror mounted into the delay stage. In CH1, a CW pilot laser output of $140\text{ }\mu\text{W}$ at $1.55\text{ }\mu\text{m}$ is amplified by a semiconductor optical amplifier (Thorlabs, EDFA100S) then split and combined by 50/50 beamsplitters (BS). One part of the interference signal is coupled into a fiber and sent back to the commercial position readout unit. A 3-port fiber circulator is used to separate the input and output beams. From the other side of the BS the signal is coupled directly onto an InGaAs photodiode (DET), which acts as a placeholder for any delay dependent setup. A chopper wheel for lock-in detection can be implemented in the focus of a one-to-one telescope and an attenuator to reduce the power in one arm.

In the Mach-Zehnder configuration (channel 1, CH1), a fiber circulator is employed to separate the output laser beam from the detected interference signal of the same port. The laser diode delivers an output power of 140 μW to each channel, which is sufficient for the normal configuration (CH2), considering a single reflection off a metal mirror and coupling back to the fiber. For the MZI, considering pump-probe setups with high optical losses, this power level is insufficient for an accurate position determination. An Erbium-doped fiber amplifier (Thorlabs, EDFA100S) was implemented to boost the CW signal resulting in an output of 80 mW in front of the interferometer. After recombination, the interfering beams are attenuated to 420 μW and coupled into the detection arm of the fiber circulator for position measurement. The other output port of the MZI beam splitter is sent onto an InGaAs photodiode (DET) for independent monitoring of the interference signal.

Optionally, a mechanical chopper with a frequency up to 10 kHz can be placed into one arm to simulate LIA detection. With additional attenuation in one arm, we can investigate the sensitivity of the position measurements for asymmetric optical losses.

2.2 Measurement control and data acquisition

Time-delay determination is based on the sinusoidal phase-modulation interferometry technique [17]. The DFB laser diode injection current is modulated at 30 MHz, which imprints a wavelength modulation on the carrier light. After demodulation at 30 MHz and its second harmonic (60 MHz) in the built-in LIA of the commercial system, two sinusoidal signals are extracted, that are phase-shifted by 90 degrees and thus, are in quadrature and dependent on the target mirror position. The quadrature signals, plotted as Lissajous figures, describe a circle in the ideal case of equal intensities and optimum alignment. At least one of the quadrature signals always exhibits high sensitivity due to high steepness. Furthermore, the direction of the movement can be followed from the sign of the phase difference between the quadrature signals. This technique requires an unbalanced interferometer and the sensitivity depends on the signal strength and working range [18]. By increasing the delay between the interferometer arms (i.e., scanning with the delay stage), the phase changes between the quadrature signals rotating the position vector in the Lissajous curve with a periodicity corresponding to an optical path delay of 1.55 μm (laser wavelength). For delays longer than 1.55 μm , the number of periods is counted. In this way, a nominal resolution of the delay measurement well below 100 pm is reached [19]. Under normal ambient conditions, mechanical and air fluctuations, as well as fast acquisition times, limit the precision to a few nanometers [20].

In measurements including the mechanical chopper, periodically blocking one of the arms results in a repeated loss of the interferometric signal. Continuous position data acquisition is achieved by (i) ensuring that the optical delay variation within one chopping period is considerably less than half the wavelength ($\lambda = 1.55 \mu\text{m}$), corresponding to a single cycle of the Lissajous graph, (ii) triggering the data acquisition of the interferometer with the chopping frequency and (iii) (manually) optimizing the timing of the chopping relative to the data acquisition. For a continuous, linear scan of the optical delay with the stage velocity ν , condition (i) imposes an upper limit on ν given by:

$$\nu \leq \frac{\lambda \cdot f}{2n} \quad (1)$$

where a factor of 2 takes into account traversing the optical path twice (in the delay line) and n is the number of points per wavelength. For scans in this paper $n \geq 19$.

The chopped photodiode signal is fed into a LIA or into an independent analog-to-digital converter (ADC) with 24-bit nominal resolution. Considering that the commercial LIA outputs have 14-bit quasi-analog outputs, the latter is advantageous for improving the SNR by reducing the digitization error. The inner clocks of the two ADCs (for position and signal detection) are synchronized by a 1 MHz reference clock signal. This common clock ensures

the correct pairing of the position data and the corresponding signal data. The data acquisition of both devices is triggered simultaneously. All output signals, namely raw quadrature signals, calculated position from the position readout unit, and signal data from the 24-bit ADC output, along with the corresponding time logs from both ADCs are transferred to the measurement control PC, where the data processing is performed (Fig. 1).

2.3 Data processing

Although the clock and start time are synchronized, there can be different delays for the devices from the trigger to the first corresponding data point. When using the LIA the averaging/filtering leads to a delay by design. By shifting one of the time axes by a single constant value for forward and backward scans, the correct shift can be found easily as it will overlay the signals scanned in the two directions optimally.

3. Results

Benchmarking measurements were performed for three different cases. First, using the MZI setup, the measured position fluctuations were corrected by the photodiode signal fluctuations for a fixed delay position. The main goal here was to demonstrate the capability of the system for highly sensitive delay measurements.

Second, for a nominally linear delay stage scan, the quality of the position signal is compared to the signal measured in the second interferometer output using an InGaAs photodiode (DET in Fig. 1) for both channels (CH1 and CH2). In this case, the effects of the chopping and intensity attenuation of one of the arms were investigated. The reproducibility of the measurements was investigated for 40 individual, 1-cm long, delay scans.

Third, the improvement of the precision with the number of averaged scans is scrutinized with a large number of short-range scans.

3.1 Delay time fluctuations at fixed position

Measuring the optical delay fluctuation at a fixed zero crossing (ZC) position demonstrates the sensitivity of the interferometric delay tracking method [21]. Furthermore, it opens a perspective towards real time optical phase measurements, like the carrier-envelope phase (CEP), if the MZI is implemented into a THz-TDS setup. Choosing a ZC position of the field amplitude in a TDS experiment, the signal fluctuations deriving from optical beam path delays can be corrected with high precision, with the remaining fluctuations originating from the CEP.

Here, we use the photodiode signal (DET) to correct the position data (CH1) which allows for the direct characterization of the method in nanometers. As we measure a complementary physical signal by the detector and the interferometer, a constant zero line is expected after the correction, affected by remaining noise.

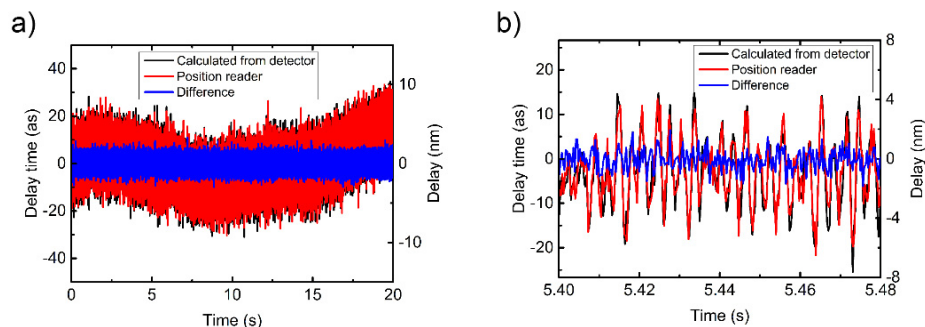


Fig. 2. The measured position (red) by the interferometer and the position calculated from the photodiode signal (black) using a linear approximation. The subtraction of the two curves gives the absolute error (blue), which can be converted to phase error using the $1.55 \mu\text{m}$ carrier wavelength. In a) a 20 seconds window is plotted and in b) a zoom to 80 ms shows the faster fluctuations. The RMS is reduced from 17.4 as (red) to 4.5 as (blue).

A 20 s long measurement was performed on a ZC position of the signal with a deviation of less than 10 nm, justifying a linear correction. The measured position fluctuations (red) and the positions were calculated from the photodiode signal (black) using just a scaling factor and setting the first point to zero. By subtraction we obtain the corrected curve (blue) around zero with a standard deviation of 1.36 nm delay, corresponding to a phase stability of 5.5 mrad at 1.55 μm over an observation time of 20 seconds. The phase data was recorded at data acquisition rates of 156 kHz. The scan over 20 seconds is shown in Fig. 2(a) and a zoomed view covering an 80-ms window in Fig. 2(b). The fluctuations visible here are due to the servo feedback of the stage. The Fourier transforms before and after correction, yielding the power spectral density of the position fluctuations, are shown in Fig. 3, together with the frequency integrated values. The external effects contributing to very slow noise (air fluctuation/some drifts) and noise up to several kHz can be reduced substantially, down to 1.36 nm RMS delay fluctuation, at a sampling rate of 156 kHz.

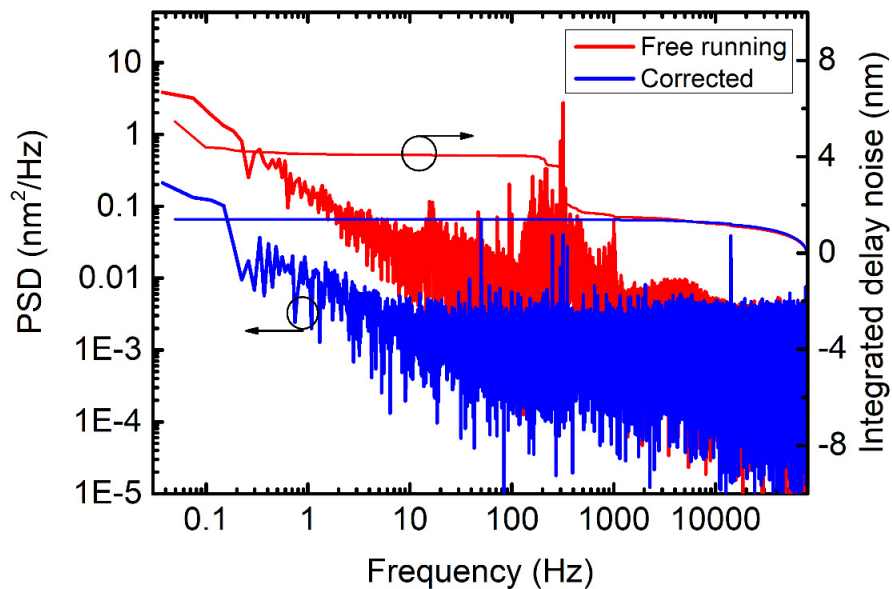


Fig. 3. Power spectral density (PSD) and integrated noise (right axes) of the position fluctuations at a zero-crossing. The correction reduces the integrated RMS delay noise from 5.25 to 1.36 nm.

3.2 Reproducibility of position for scanning operations

Depending on the application, it can be important to focus on the temporal and/or the spectral domain. The dynamic range and signal to noise ratio are important merits in both domains, but the conversion between the temporal and spectral domain values requires a careful treatment which is beyond the scope of this paper (e.g. the dynamic range in the spectral domain depends on the scanning range, the time step or the number of averages of full time-domain traces [22]). Furthermore, the impact of delay line noise becomes more essential for higher frequencies, because the same amount of jitter has a stronger effect on the signal where the steepness is higher [10]. In the following, we focus on a comparison of the position tracking measurement with the commercial Michelson-interferometer-based position readout (CH2/Ref.) and the MZI configuration (CH1).

Fourty scans were recorded for each setting, pairing the photodiode signal (DET) data with the corresponding position data of CH1 and CH2, respectively. The quality of the measurement was verified in the time domain by comparing the deviation of the position of all zero-crossings of different scans in a 33-ps window (1 cm delay). All the scans were recorded with 0.2 mm/s scanning speed, 5 kHz chopping frequency, and 156 kHz sampling rate for the signal while only one position point was measured during each chop with 1/156 ms acquisition time. The zero-crossing positions are those in which the interferometric signal (DET) crosses the mean value of its modulation. To determine each position, linear interpolation between the acquired points directly above and below the mean value is used. For each of the almost 13000 crossings, the standard deviation of its position in 40 scans is calculated (zero crossing fluctuation).

In Fig. 4(a) a comparison between tracking only the stage movement (CH2/Ref.) and tracking the whole interferometer (CH1) is shown. As drifts within the interferometer affect the first, all scans were shifted in position such that the sinusoidal signals had the lowest deviation in phase in a 1-ps window [at 22 ps delay in Fig. 4(a)]. As expected, the chopper causes additional fluctuations and increases the mean repeatability of all ZCs from 62 to 127 as (18.6 to 38.2 nm). The corrected case however, shows a dramatically improved repeatability, with 8.2 as and 11.2 as (2.46/3.36 nm) for the un-chopped and chopped case respectively. The difference between chopped and not chopped operation is with less than 3 as very small (The observed differences seem to be caused partially by different calibrations of the PicoScale device). Comparing these values to the stationary case we notice an increase by almost a factor of two to the instrument limit with these settings, due to the moving stage introducing additional fluctuations. Overall, the reproducibility of single scans with about 10 as per 2 points (to calculate the ZC) is remarkable.

In this measurement, the power coupled back to the PicoScale detector was attenuated from 33 mW to 420 μ W. To test the performance at even further attenuation and also asymmetric power in the interferometer arms, one arm was attenuated by a neutral density filter by a factor of 20. The comparison only for CH1 between the attenuated case and the ideal case is shown in Fig. 4(b). The mean values are 14 and 16 as (4.2 and 4.8 nm) which is only slightly worse than without the filter. A significant contribution to this change is attributed to the reduction of the signal-to-noise ratio of the sinusoidal signal and not due to a reduction of the quality of the position data.

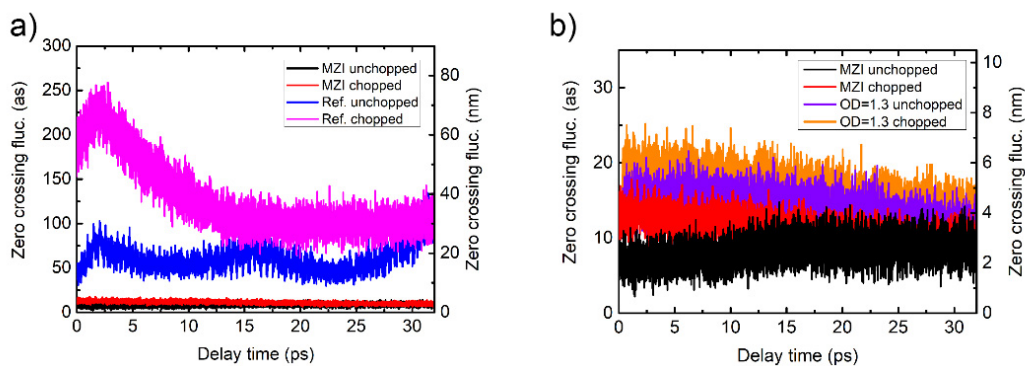


Fig. 4. Comparison of the position reproducibility of the MZI and the reference setup in a) and only for the MZI with and without attenuating one arm in b). In each case 1 cm long delay scans were performed with chopped and not chopped interferometer arm.

3.3 Long-term stability

The results presented so far were based on single scans with data and position acquired in 1/156 ms per point. While the manufacturer claims down to a few pm for longer integration times, it is informative to test how many scans can be averaged to further improve the reproducibility between averaged scans in the same way as done in Fig. 4(a). For these scans the velocity was 0.1 mm/s, with a delay of 600 μm containing 374 ZCs, and the chopper frequency was 5 kHz. Figure 5 shows an Allan deviation-like measurement. For each scan the ZCs positions are evaluated. Each ZC position is then averaged over a number of consecutive scans. This procedure is repeated for the same number of scans recorded immediately thereafter. The standard deviation for all 374 ZCs of these two samples is calculated and the average over all 374 forms the Allan deviation of these two samples. In Fig. 5 the mean and the standard deviation of 10 consecutive Allan deviations are plotted. The behavior till 32 scans (76 s) is almost noise limited, until the system starts to be affected by small drifts. The optimal value is reached for roughly 100 averages with an expected reproducibility of about half an attosecond (0.17 nm). This result makes this setup also very interesting whenever sub-attosecond precision is required. Notably, this averaging procedure is still allows for quite fast acquisition rates, with the cumulative acquisition time for one ZC for 100 scans is still only 1.3 ms.

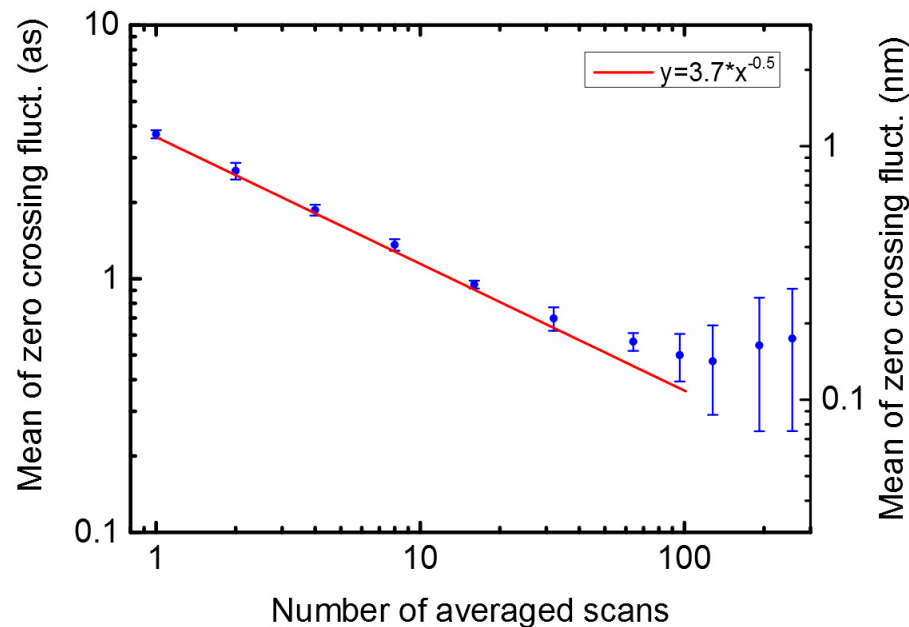


Fig. 5. The temporal stability/reproducibility of the position measurement is evaluated and plotted in an Allan deviation-like manner.

4. Conclusion and perspectives

In this paper, we present an interferometric delay tracking method for high precision position detection and real-time correction in ultrafast pump-probe experiments using conventional, mechanical delay lines. A commercial fiber-based Michelson interferometer with nominally picometer position resolution was adapted for a typical Mach-Zehnder arrangement of pump-probe setups. Furthermore, according to our best knowledge this is the first MZI positioning setup combined with mechanical chopping for lock-in amplifier detection. Applying our IDT in a test setup we demonstrate the capability to track and compensate noise sources up to

several kHz with a root-mean-square delay accuracy of 1.4 nm at 156 kHz sampling rate. In direct comparison to tracking the stage position only, the positioning fluctuations of 40 scans were an order of magnitude lower when tracking the absolute delay interferometrically and over a 1-cm delay (with 2.5 nm and 3.3 nm when chopped) are almost as good as in the stationary case (1.36 nm). The implementation of the applied system into THz-TDS opens the way for more accurate measurements, which can be combined with lock-in detection. Furthermore, we demonstrate that with higher acquisition time sub-attosecond reproducibility for chopped delay scans is possible, which makes this setup also interesting for slower scans requiring higher precision. With an amplified beam, losses at 1.55 μm wavelength in real setups can be compensated, making this approach very versatile for most pump-probe setups.

Funding

Munich Centre for Advanced Photonics (www.munich-photonics.de), a DFG-funded Cluster of Excellence.

Acknowledgments

We thank Ferenc Krausz for helpful discussions.

Disclosures

The authors declare that there are no conflicts of interest related to this article.

References

1. P. B. Corkum and F. Krausz, "Attosecond science," *Nat. Phys.* **3**(6), 381–387 (2007).
2. M. Hentschel, R. Kienberger, C. Spielmann, G. A. Reider, N. Milosevic, T. Brabec, P. Corkum, U. Heinzmann, M. Drescher, and F. Krausz, "Attosecond metrology," *Nature* **414**(6863), 509–513 (2001).
3. R. Gebs, G. Klatt, C. Janke, T. Dekorsy, and A. Bartels, "High-speed asynchronous optical sampling with sub-50fs time resolution," *Opt. Express* **18**(6), 5974–5983 (2010).
4. J. Xu, B. Globisch, C. Hofer, N. Lilienfein, T. Butler, N. Karpowicz, and I. Pupeza, "Three-octave terahertz pulses from optical rectification of 20 fs, 1 μm 78 MHz pulses in GaP," *J. Phys. At. Mol. Opt. Phys.* **51**, 154002 (2018).
5. M. Chini, H. Mashiko, H. Wang, S. Chen, C. Yun, S. Scott, S. Gilbertson, and Z. Chang, "Delay control in attosecond pump-probe experiments," *Opt. Express* **17**(24), 21459–21464 (2009).
6. A. Yabushita, Y. H. Lee, and T. Kobayashi, "Development of a multiplex fast-scan system for ultrafast time-resolved spectroscopy," *Rev. Sci. Instrum.* **81**(6), 063110 (2010).
7. M. J. Feldstein, P. Vöhringer, and N. F. Scherer, "Rapid-scan pump-probe spectroscopy with high time and wave-number resolution: optical-Kerr-effect measurements of neat liquids," *J. Opt. Soc. Am. B* **12**(8), 1500 (1995).
8. W. Withayachumnankul, H. Lin, S. P. Micken, B. M. Fischer, and D. Abbott, "Analysis of measurement uncertainty in THz-TDS," *Proc. SPIE* **6593**, 659326 (2007).
9. A. Rehn, D. Jahn, J. C. Balzer, and M. Koch, "Periodic sampling errors in terahertz time-domain measurements," *Opt. Express* **25**(6), 6712–6724 (2017).
10. O. Schubert, M. Eisele, V. Crozatier, N. Forget, D. Kaplan, and R. Huber, "Rapid-scan acousto-optical delay line with 34 kHz scan rate and 15 as precision," *Opt. Lett.* **38**(15), 2907–2910 (2013).
11. C. Li, G.-Q. Liao, and Y.-T. Li, "Non-scanning systems for far-infrared radiation detection from laser-induced plasmas," *High Power Laser Sci. Eng.* **3**(May), 15 (2015).
12. D. Brida, C. Manzoni, and G. Cerullo, "Phase-locked pulses for two-dimensional spectroscopy by a birefringent delay line," *Opt. Lett.* **37**(15), 3027–3029 (2012).
13. J. Köhler, M. Wollenhaupt, T. Bayer, C. Sarpe, and T. Baumert, "Zeptosecond precision pulse shaping," *Opt. Express* **19**(12), 11638–11653 (2011).
14. J. Réhault, F. Crisafi, V. Kumar, G. Ciardi, M. Marangoni, G. Cerullo, and D. Polli, "Broadband stimulated Raman scattering with Fourier-transform detection," *Opt. Express* **23**(19), 25235–25246 (2015).
15. D. Molter, M. Trierweiler, F. Ellrich, J. Jonuscheit, and G. Von Freymann, "Interferometry-aided terahertz time-domain spectroscopy," *Opt. Express* **25**(7), 7547–7558 (2017).
16. SmarAct PicoScale, *User Manual*, (SmarAct, 2017).
17. O. Sasaki and H. Okazaki, "Sinusoidal phase modulating interferometry for surface profile measurement," *Appl. Opt.* **25**(18), 3137–3140 (1986).
18. M. Zhang, C. Ni, Y. Zhu, C. Hu, J. Hu, L. Wang, and S. Ding, "Sinusoidal phase-modulating laser diode interferometer for wide range displacement measurement," *Appl. Opt.* **56**(20), 5685–5691 (2017).
19. SmarAct Application Note, *PicoScale Stability and Resolution*, (SmarAct, 2017).

20. W. Gao, S. W. Kim, H. Bosse, H. Haitjema, Y. L. Chen, X. D. Lu, W. Knapp, A. Weckenmann, W. T. Estler, and H. Kunzmann, "Measurement technologies for precision positioning," *Manuf. Technol.* **64**(2), 773–796 (2015).
21. D. Jahn, S. Lippert, M. Bisi, L. Oberto, J. C. Balzer, and M. Koch, "On the influence of delay line uncertainty in thz time-domain spectroscopy," *J. Infrared Millim. Terahertz Waves* **37**(6), 605–613 (2016).
22. J. Xu, T. Yuan, S. Mickan, and X. C. Zhang, "Limit of spectral resolution in terahertz time-domain spectroscopy," *Chin. Phys. Lett.* **20**(8), 1266–1268 (2003).